Hindawi Publishing Corporation
International Journal of Photoenergy
Volume 2013, Article ID 439079, 9 pages
http://dx.doi.org/10.1155/2013/439079

Research Article

Preparation of N-TiO_2 Using a Microwave/Sol-Gel Method and Its Photocatalytic Activity for Bisphenol A under Visible-Light and Sunlight Irradiation

Chung-Hsin Wu,[1] Chao-Yin Kuo,[2] Chin-Jung Lin,[3] and Peng-Ke Chiu[2]

[1] *Department of Chemical and Materials Engineering, National Kaohsiung University of Applied Sciences, 415 Chien-Kung Road, Kaohsiung 80778, Taiwan*
[2] *Department of Safety Health and Environmental Engineering, National Yunlin University of Science and Technology, Yunlin 64002, Taiwan*
[3] *Department of Environmental Engineering, National Ilan University, Ilan 26041, Taiwan*

Correspondence should be addressed to Chung-Hsin Wu; wuch@kuas.edu.tw

Received 20 November 2012; Revised 4 January 2013; Accepted 13 January 2013

Academic Editor: Mahmoud M. El-Nahass

This study applied the microwave/sol-gel method to prepare nitrogen-doped TiO_2 (N-TiO_2). The N-TiO_2 was immobilized in glass balls to form N-TiO_2/glass beads and applied to degrade Bisphenol A (BPA) under visible-light and sunlight irradiation. The characteristics of the prepared photocatalysts were analyzed by X-ray diffraction (XRD), UV-Vis spectroscopy, Fourier transform infrared spectroscopy (FTIR), and X-ray photoelectron spectroscopy (XPS). Experimental results demonstrate that the percentage of anatase increased as the amount of N in N-TiO_2 increased. Compared with the undoped TiO_2 (420 nm), spectra show that the absorption edge shifted to a longer wavelength (445 nm) after N doping. The XPS characterization confirms the substitution of crystal lattice O to N species in N-TiO_2, forming Ti–O–N and N–Ti–O. With an increased N/Ti ratio, photodegradation efficiency increased and then decreased; moreover, the optimal amount for N doping was determined as an N/Ti mole ratio of 0.08 (0.1 NT). The efficiency of 0.1 NT in doing BPA photodegradation was greater than that of Degussa P25. After reaction for 61 min, the mineralization percentage of 0.1 NT under visible-light irradiation reached 41%. Photocatalyst efficiency decreased as the number of repeats increased in the visible-light/N-TiO_2 system; however, these systems were stable during reaction.

1. Introduction

Bisphenol A (BPA), a monomer of various polymeric materials, is utilized primarily to produce epoxy resins and polycarbonate products [1]. Recent studies have shown that BPA can leach out of the plastic lining of food cans [2]. Due to its continued use in household and commercial products, large amounts of BPA have been released into aquatic environments. Based on its ability to disrupt endocrine function, the presence of BPA in aquatic environments and its potential adverse impacts on ecological and public health have garnered increased attention. Hence, researchers must develop effective remediation techniques that degrade BPA in wastewater.

Advanced oxidation processes (AOPs) are effective approaches for degrading and reducing recalcitrant wastewater loads from industrial processes. Significant progress has been made in developing AOPs for BPA degradation in recent years. Notably, AOPs involve primarily the generation of a very powerful nonselective oxidizing agent, the hydroxyl radical, which destroys pollutants. Because of its nontoxicity, photochemical stability, and reasonable cost, TiO_2-based photocatalysis has been studied extensively for wastewater treatment. In ultraviolet light (UV)/TiO_2-based systems, TiO_2 particles absorb UV energy that is greater than the TiO_2 band gap and form an electron and hole pair in the conduction band and valence band, respectively. The positive holes oxidize water molecules into hydroxyl

radicals, and negative electrons reduce molecular oxygen to yield superoxide radical anions. These positive holes, hydroxyl radicals, and superoxide radical anions are the dominant oxidizing species in UV/TiO_2 systems. However, rapid unfavorable recombination of photo-produced electrons and holes in TiO_2 markedly reduces the photocatalytic efficiency. Additionally, TiO_2 can only be photoexcited by UV; hence, developing photocatalysts that make full use of solar energy is necessary. Several investigations have synthesized sulfur-doped TiO_2 (S-TiO_2) [3, 4] and nitrogen-doped TiO_2 (N-TiO_2) [5–7], which extend the spectral response of TiO_2 into the visible light region, thereby enhancing the photocatalytic activity of TiO_2.

Various studies have used different AOPs to treat BPA, including ozone [8, 9], UV/ozone [8], UV/TiO_2 [10–14], visible-light/TiO_2 [15–17], sunlight/TiO_2 [18], UV/Zr-TiO_2 [19], UV/Pt-TiO_2 [12], UV/Au-TiO_2 [13], Fenton [14, 20, 21], UV/Fenton [20], ultrasound (US) [22, 23], US/Fenton [21], US/TiO_2/Fe^{2+} [14], visible-light/N-TiO_2 [17], and visible-light/C-N-TiO_2 [24, 25] systems. Notably, BPA can be readily eliminated by the US process (~90 min); however, over 80% of the total organic carbon (TOC) remained in the solution after US irradiation for 9 h [23]. Additionally, the US/Fenton system increased the BPA degradation rate as compared to the Fenton system only [21]. The Zr-doped [19], Au-doped [13], and Pt-doped [12] TiO_2 photocatalysts had better photocatalytic efficiency than pure TiO_2 during the degradation of BPA under UV irradiation. Wang and Lim [24], who applied visible-light to photoexcite N-TiO_2 and Degussa P25 for BPA degradation, demonstrated that the BPA removal percentage after reaction for 2 h was 29% and 5%, respectively. The BPA photodegradation rate under visible-light irradiation was as follows: N-TiO_2 > Degussa P25 > undoped TiO_2 [17]. Since Sojic et al. [26] suggested that nonmetals are more efficient dopants than metals for TiO_2, TiO_2 and N-TiO_2 were selected as photocatalysts for BPA degradation in this study.

A slurry reactor system was used in most experiments, in which TiO_2 particles were suspended in the form of a colloid and utilized as a photocatalyst. However, the required separation of the ultrafine photocatalyst particles from the treated liquid hindered the wide application of slurry photocatalytic reaction systems. Only Nakashima et al. [10] and Wang et al. [15] have used a UV/immobilized TiO_2 system to degrade BPA. No study has investigated the BPA photodegradation by visible-light/immobilized TiO_2 and sunlight/immobilized TiO_2 systems. This study synthesizes TiO_2 and N-TiO_2 using the microwave/sol-gel method and immobilizes photocatalysts on glass balls to form fixed beads. The objectives of this study are to (i) identify the characteristics of prepared TiO_2 and N-TiO_2 particles, (ii) compare the photocatalytic activity of TiO_2 and N-TiO_2 for BPA degradation under visible-light and sunlight irradiation under an immobilized condition, (iii) determine the effects of photocatalyst dosage and amount of N doping, and (iv) investigate repeated usability of the visible-light/immobilized N-TiO_2 system for BPA degradation.

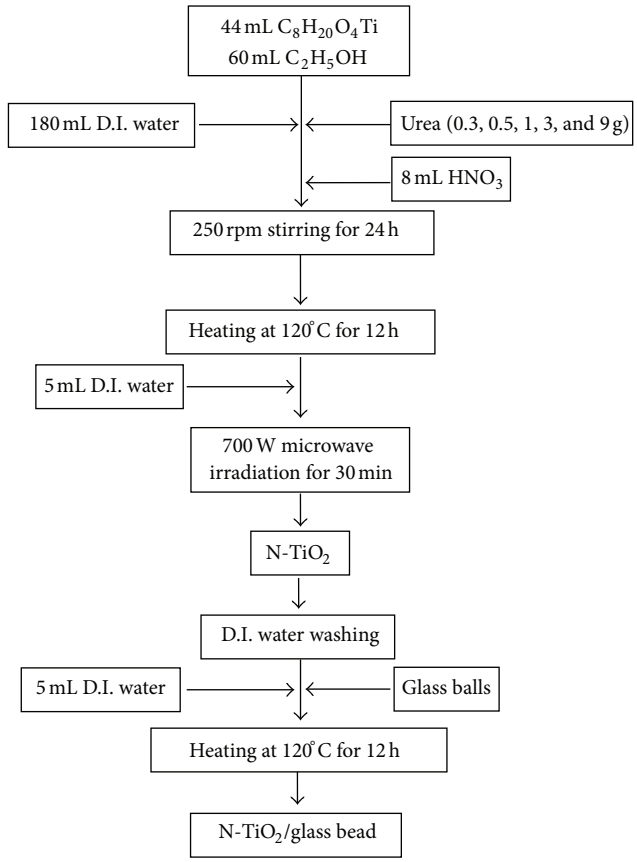

Figure 1: Flowchart for the procedure used to prepare immobilized N-TiO_2/glass bead.

2. Materials and Methods

2.1. Materials. The Ti and N source was ethyl titanate ($C_8H_{20}O_4Ti$) and urea, respectively (Merck). Ethanol was applied as a modulator when preparing TiO_2. The parent compound, BPA, was obtained from Sigma-Aldrich (purity > 99%). Solution pH was adjusted using HNO_3 and NaOH. Degussa P25 was utilized as the standard material to compare photocatalytic activity of prepared TiO_2 and N-TiO_2 for BPA photodegradation. All chemicals were analytical reagent grade and used as received.

2.2. Preparation of the Immobilized TiO_2/Glass Bead and N-TiO_2/Glass Bead. Figure 1 presents a flowchart of the procedure used to prepare immobilized N-TiO_2/glass beads. In preparing N-TiO_2, 44 mL $C_8H_{20}O_4Ti$ was mixed with 60 mL ethanol and then mixed further with 180 mL deionized water. An appropriate amount of urea (0.3, 0.5, 1, 3, and 9 g) was added. Then, 8 mL HNO_3 was added, and the entire mixture was stirred at 250 rpm for 24 h. After gel formation, the batch was dehydrated at 120°C. Dehydrated gels were first ground, and 5 mL deionized water was then added. The resulting gels were irradiated in a 700 W microwave (2425–2475 MHz) for 30 min to generate N-TiO_2 powder. Glass balls (5 mm in diameter) were etched to generate a rugged surface

in 5 M NaOH (100°C) for 5 h. The N-TiO_2 and pretreated glass balls were washed 5 times with deionized water. The clean and etched glass balls were immersed in a 5% (w/v) N-TiO_2 solution. The glass balls were conditioned at 120°C for 12 h to form immobilized N-TiO_2/glass beads. The mole ratio of N/Ti for the obtained N-TiO_2/glass beads under addition of 0.3, 0.5, 1, 3, and 9 g urea was 0.05, 0.08, 0.17, 0.5, and 1.5, respectively, and these N-TiO_2/glass beads are denoted as 0.05 NT, 0.1 NT, 0.2 NT, 0.5 NT, and 1.5 NT herein, respectively. If no urea was added, the TiO_2/glass beads (T) were produced. The 5% (w/v) Degussa P25 solution was also calcined with pretreated glass balls at 120°C for 12 h to form a Degussa P25/glass beads (P).

2.3. Characterization. The crystallinity of photocatalysts was analyzed by X-ray diffraction (XRD) using CuKα radiation (Bruker AXS). Accelerating voltage and applied current were 40 kV and 30 mA, respectively. The XRD patterns were recorded as 2θ values at 10–80° and a scanning speed of 3°/min. The UV-Vis spectroscopy (Jasco V-670) method was applied to profile the absorbance spectrum of photocatalysts at wavelengths of 200–800 nm. The UV-Vis diffuse reflectance spectra were used to calculate photocatalyst band gap energy. Functional groups of photocatalysts were identified by Fourier transform infrared spectroscopy (FTIR) using a Spectrum One and AutoIMAGE system (Perkin Elmer) via the KBr pressed disc method. An inductively coupled plasma-optical emission spectrometer (ICP-OES, Optima 2100DV) was utilized to measure the TiO_2 concentration in effluent. The X-ray photoelectron spectroscopy (XPS) measurements were performed using a Vacuum Generator ESCALAB MKII photoelectron spectrometer (East Grinsted) with an ALKR 1, 2 (1486.6 eV) X-ray source. Binding energies of photoelectrons were determined based on the assumption that carbon 1s electrons were at 284.5 eV. The BPA concentration was measured using a high-performance liquid chromatograph (HPLC) with a UV detector (Agilent Technologies). The UV detector was set to a wavelength of 197 nm. Separations were performed using a Supelcosil C18 column (Supelco). The mobile phase was Milli-Q water and CH_3CN (40 : 60 v/v) at a flow rate of 0.5 mL/min. Injection volume was 20 μL. The decrease in TOC, measured using an O.I. 1010 TOC analyzer, indicated a BPA mineralization.

2.4. Photodegradation of BPA. The photocatalytic reactor (Figure 2) consisted of 4 30 cm long quartz tubes and 5 visible-light lamps. The external diameter of each tube was 1.2 cm, and the internal diameter was 1 cm. In total, 10–40 photocatalyst/glass balls were filled into each quartz tube before 10 mg/L of BPA solution was introduced into the system using a peristaltic pump. The photocatalyst dosage in the photocatalytic reactor was 1.7–6.7 g/L. The optimal experimental pH for BPA degradation in the sunlight/TiO_2 system was 6, because a chemical treatment was not needed, including a neutralization process [18]. Hence, the initial solution pH was adjusted to 6 herein. The flow rate of the BPA solution was maintained at 1.5 mL/min. The column photoreactor was irradiated with 410 nm visible light (8 W, Philips) at room temperature. The quartz tubes were arranged at equal distances around the 5 lamps. Moreover, the system was analyzed under sunlight in selected experiments for comparison purposes. The intensity of visible light and sunlight was 2.88 and 23.46–24.06 mW/cm^2, respectively. Some experiments were performed in triplicate, and average values are reported.

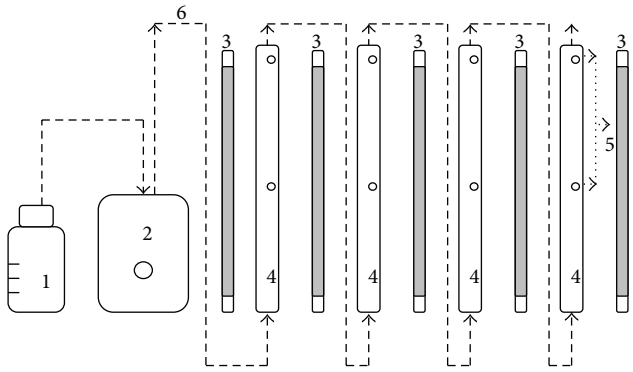

Figure 2: The scheme of the column photoreactor ((1) storage tank, (2) peristaltic pump, (3) light source, (4) column, (5) sampling pores, and (6) connection tube).

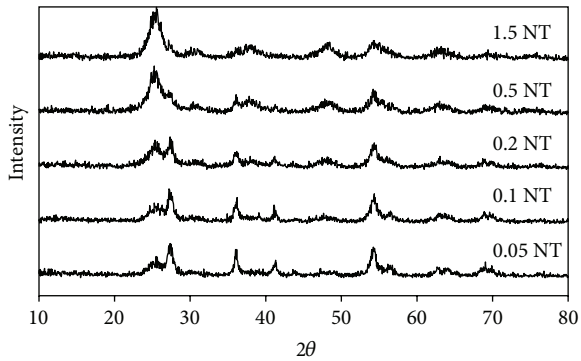

Figure 3: XRD pattern of photocatalysts.

3. Results and Discussion

3.1. Physical Characterization of Photocatalysts. Figure 3 shows XRD patterns of N-TiO_2 samples with differing N content. The 2θ peaks at 25.5°, 37.8°, and 48.1° indicate anatase-type TiO_2, and those at 27.5° and 36.1° indicate rutile-type TiO_2. No N-derived peak was detected in any pattern. Anatase is considered the photoactive form, whereas rutile exhibits low photocatalytic activity. However, the source of the activity difference remains unknown. The ratio of anatase to rutile in photocatalysts was calculated using the following well-known formula [27]:

$$X_A\,(\%) = \left(\frac{I_A}{I_A + 1.265 I_R}\right) \times 100, \quad (1)$$

Table 1: Characteristics of the prepared photocatalysts.

Photocatalysts	Crystalline phase		Absorbed wavelength (nm)	Band gap (eV)
	Anatase (%)	Rutile (%)		
P	82.1	17.9	413	3.00
T	38.7	61.3	420	2.95
0.05 NT	33.2	66.8	429	2.89
0.1 NT	34.5	65.5	438	2.83
0.2 NT	41.9	58.1	445	2.79
0.5 NT	63.0	37.0	445	2.79
1.5 NT	73.6	26.4	445	2.79

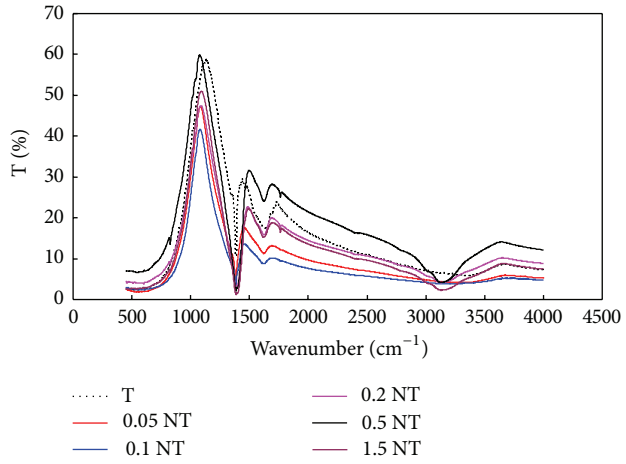

Figure 4: FTIR spectra of different photocatalysts.

where X_A is the fraction of anatase in the photocatalyst, I_A is the (101) peak intensity of anatase at 25.5°, I_R is the (110) peak intensity of rutile at 27.5°, and 1.265 is the scattering coefficient. Degussa P25, which is a standard material in photocatalytic reactions, contains anatase and rutile phases at a ratio of roughly 3 : 1 (Table 1). The synthesized TiO_2 particles have less anatase than Degussa P25. As the amount of N in N-TiO_2 increases, the ratio of anatase to rutile increases (Table 1). The XRD diagrams indicate that N doping retards the transformation of TiO_2 phase from anatase to rutile. This retardation of phase transformation may be due to stabilization of the anatase phase by surrounding N ions via the formation of Ti–O–N bonds. Ma et al. [7] obtained similar analytical results for samarium doping.

The electronic structure of a photocatalyst affects its optical absorption and migration of light-induced electrons and holes. The band gap of the photocatalyst was calculated using the formula $Eg = 1240/\lambda_g$, where λ_g is the wavelength value corresponding to the intersection point of the vertical and horizontal section of spectra. The impact of N doping on the band gap of N-TiO_2 is investigated (Table 1). Compared with undoped TiO_2 (420 nm), the spectra show the absorption edge shifting to a longer wavelength (445 nm) after N doping. All N-TiO_2 had high photoabsorption capacity in the range of UV light to visible light, and the number of photo-generated electrons and holes to participate in the photocatalytic reaction was increased; additionally, the significant narrowing of the band gap is of great importance for practical applications of N-TiO_2 since N-TiO_2 can be activated by sunlight (Table 1).

The band gap energy of Degussa P25 was 3.00 eV (Table 1), and this value was the same as that determined by Silveyra et al. [6] and Liu et al. [28]. The band gap energy of TiO_2 decreased from 2.95 eV to 2.79 eV via N doping (Table 1). In previous studies, the band gap energy of TiO_2 decreased from 3.01 eV to 2.88 eV via N doping [6]; moreover, the same trend (band gap energy of TiO_2 decreasing from 3.09 eV to 2.84 eV) was also obtained by Ma et al. [7]. Hussain et al. [29] and Wang et al. [30] indicated that the band gap value of a photocatalyst decreases as the amount of dopant increases. Notably, N-doping was effective in decreasing the band gap of TiO_2 by generating an isolated N 2p narrow band above the O 2p valence, which formed by incorporating N atoms into the TiO_2 lattice [5].

Figure 4 shows the FTIR spectra of different photocatalysts obtained with different urea concentrations. Three major absorbance peaks were observed at 1384, 1625, and 3130 cm^{-1}. The absorption peak at 1625 cm^{-1} belongs to the Ti-O structure [29, 31, 32]. The board absorption band at 3100–3300 cm^{-1} was characteristic of OH^- stretching vibrations on the photocatalyst surface [31]. The peak at 1384 cm^{-1} corresponds to the surface adsorbed NO_3^- molecules [33]. Adsorption of NO_3^- molecules onto prepared photocatalysts can be attributed to adding HNO_3 during photocatalyst preparation. Hu et al. [34] demonstrated that hydrolysis of $TiCl_4$ in a urea solution led to chemisorption of NH_3 molecules on the TiO_2 surface and to the formation of nitride species in the TiO_2 lattice. However, N atoms incorporated into the TiO_2 crystal lattice were not identified by FTIR analysis in this study.

The XPS characterization further confirms the substitution of crystal lattice O for N species in N-TiO_2. Figure 5 shows XPS spectra for the N 1s region of N-doped TiO_2 for 0.05 NT, 0.1 NT, 0.2 NT, and 0.5 NT, respectively, and their fitting curves. After curve fitting, two peaks with binding energies of 399 and 401 eV were identified. The peak at 399 eV has been attributed to anionic N in N–Ti–O linkages by many researchers [5, 35]. Another peak at a higher binding energy of 401 eV for the N 1s region of N-TiO_2 was attributed to oxidized N in Ti–O–N. Xing et al. [36] indicated that this oxidized N in Ti–O–N is chemically adsorbed onto the

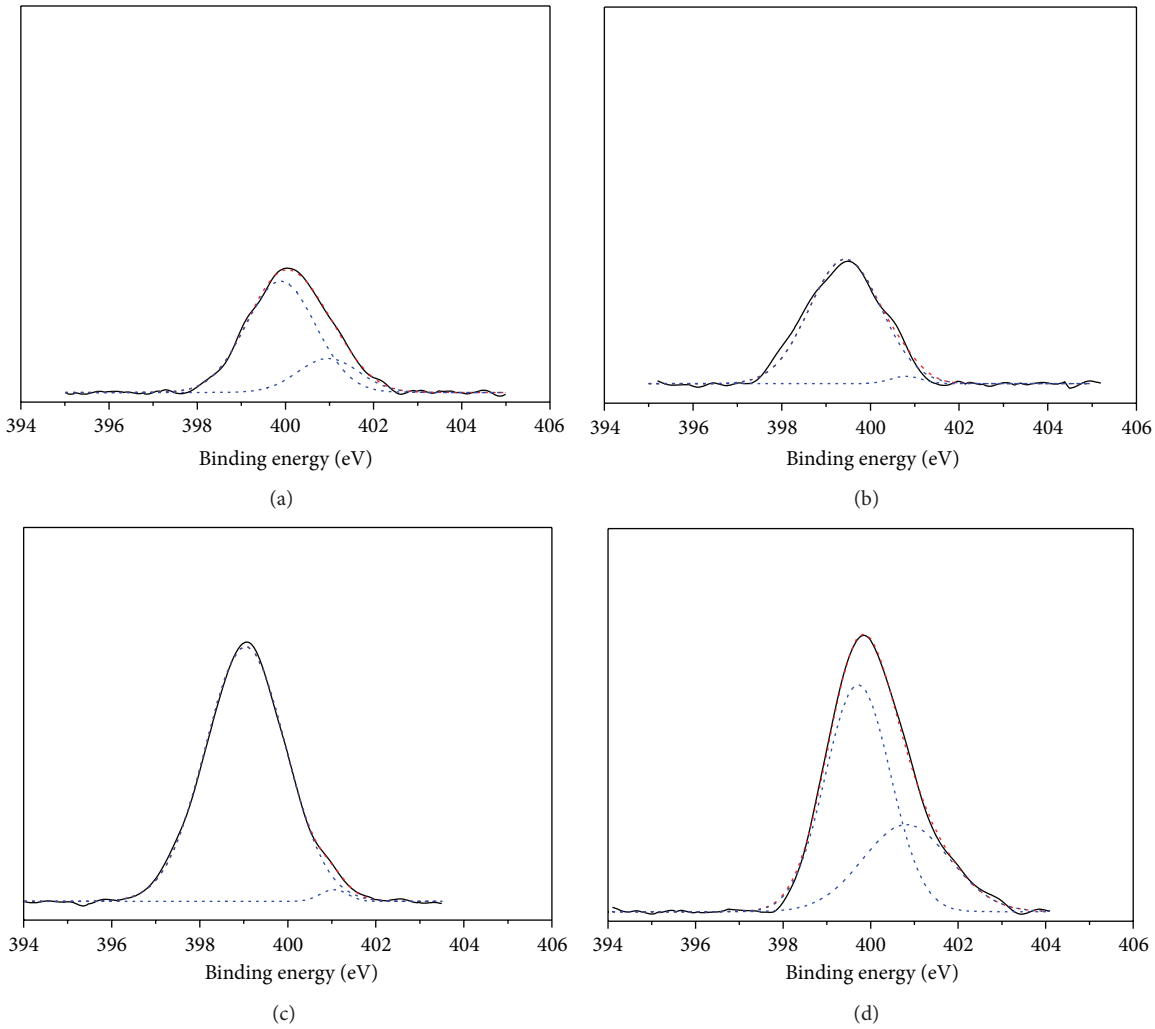

Figure 5: Fitting XPS spectra for N 1s region of N-doped TiO_2 for (a) 0.05 NT, (b) 0.1 NT, (c) 0.2 NT, and (d) 0.5 NT.

catalyst surface and appears at a high binding energy of 401 eV in N 1s XPS spectra. The Ti 2p region of 0.2 NT shows that the Ti $2p^{3/2}$ and Ti $2p^{1/2}$ core levels in N-TiO_2 appear at 458.5 and 464.3 eV, respectively (Figure 6). The binding energies of Ti $2p^{3/2}$ and Ti $2p^{1/2}$ after N doping decreased when compared with that of pure TiO_2 (Ti $2p^{3/2}$ appears at 459.1 eV, and Ti $2p^{1/2}$ appears at 465.0 eV). The possible reason is that N is incorporated into the lattice and substitutes for O, and the lower electronegativity of N compared with that of O leads to electron transformation from N to Ti to increase electron density on Ti [31, 37]. The XPS spectra of the O 1s region of 0.2 NT have two peaks after curve fitting (Figure 7). The peak at 529.8 eV is attributed to O 1s in Ti–O linkages of TiO_2. Another peak at 531.5 eV is attributed to the presence of Ti–O–N bonds [38, 39]. The peaks at about 529.8 and 531.5 eV indicate the presence of two oxygen states, Ti–O–Ti and Ti–O–N, respectively. Based on these observations, we conclude that the chemical states of N-doped TiO_2 may coexist as N–Ti–O (N1) and Ti–O–N (N2). According to the XPS spectra, different fitting peak nitrogen percentages in the TiO_2 were calculated in relation to titanium (Table 2). The highest N1/N2 ratio was 0.2 NT; additionally, the highest N-doping concentration was 0.5 NT (Table 2). Xing et al. [36] indicated that when the N/Ti value increases, the ratio of N1/N2 increases first and then decreases; this study obtained a similar trend.

Table 2: Nitrogen doping ratio of 0.05 NT, 0.1 NT, 0.2 NT, and 0.5 NT.

	0.05 NT	0.1 NT	0.2 NT	0.5 NT
N1/Ti	0.00200	0.00249	0.00546	0.00384
N2/Ti	0.00053	0.00007	0.00009	0.00196
N1/N2	3.8	35.5	63.5	2.0
Total doping N	0.15%	0.16%	0.33%	0.35%

N1 refers to N in N–Ti–O linkages. N2 refers to N in Ti–O–N.

3.2. Effects of Photocatalyst Dosage and Amount of N Doping in TiO_2. Under the addition of 6.7 g/L photocatalyst, the adsorption of BPA by T, P, 0.05 NT, 0.1 NT, 0.2 NT, 0.5 NT,

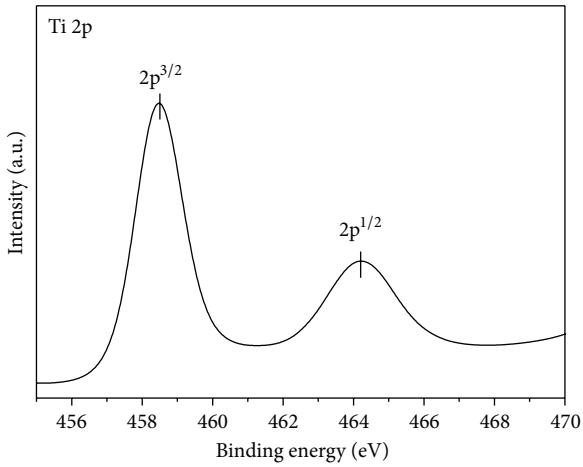

Figure 6: XPS spectra for Ti 2p region of 0.2 NT.

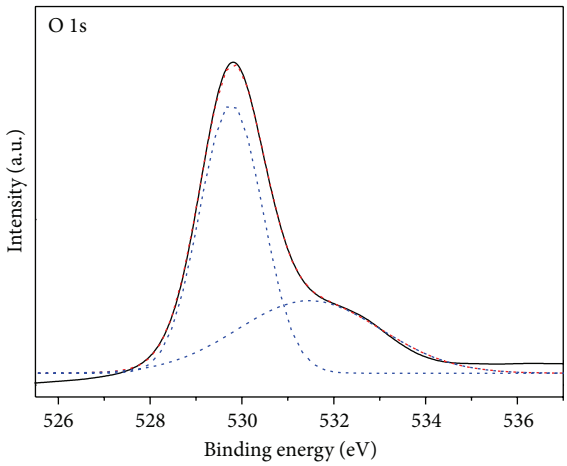

Figure 7: XPS spectra for O 1s region of 0.2 NT.

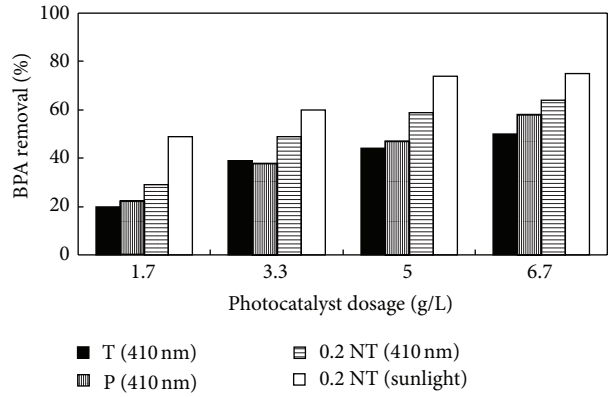

Figure 8: BPA removal percentage at different photocatalyst dosages (BPA = 10 mg/L, pH = 6, and time = 61 min).

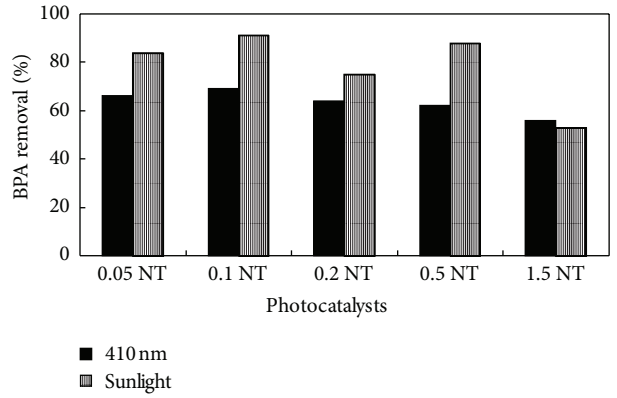

Figure 9: BPA removal percentage at different N-TiO_2 (BPA = 10 mg/L, pH = 6, time = 61 min, and photocatalyst = 6.7 g/L).

and 1.5 NT after reaction for 61 min was 25%, 5%, 15%, 12%, 10%, 11%, and 12%, respectively. After reaction for 61 min, the photolysis of BPA by 410 nm visible light, and sunlight irradiation was 4% and 29%, respectively. The BPA removal was ineffective by photocatalyst adsorption and photolysis. Figure 8 shows the BPA removal percentages under different photocatalyst dosages. Under 410 nm visible-light irradiation on 0.2 NT, BPA removal at 1.7, 3.3, 5.0, and 6.7 g/L was 29%, 49%, 59%, and 64%, respectively; additionally, for 0.2 NT under sunlight irradiation, BPA removal was 49%, 60%, 74%, and 75%, respectively. The BPA degradation efficiency increased as the amount of photocatalyst increased. This increase in efficiency is due to an increased total surface area, namely, the number of active sites, available for the photocatalytic reaction as the photocatalyst dosage increased [18]. Under the same photocatalyst dose, BPA removal percentage for 0.2 NT was higher than that for T and P. This study demonstrates that photocatalytic activity of TiO_2 was enhanced by N doping.

Figure 9 shows the effects of the N doping dosage in TiO_2 for BPA removal. Under 410 nm visible-light irradiation, BPA removal of 0.05 NT, 0.1 NT, 0.2 NT, 0.5 NT, and 1.5 NT was 66%, 68%, 64%, 62%, and 56%, respectively; moreover, under sunlight irradiation, BPA removal was 84%, 91%, 75%, 88%, and 53%, respectively. With the increase in the N/Ti ratio (ratio of urea to TiO_2), photodegradation efficiency first increases and then decreases (Figure 9). The effects of the N doping dosage in catalyst for photodegradation efficiency were similar to those observed by Xing et al. [36]. A high doping concentration of N increases the energy shift due to a significant overlap of N and O states, leading to a narrow band gap in N-TiO_2 (Table 1). An optimal amount of C, N, and/or S dopant exists at which they can synergistically serve as electron traps that inhibit recombination of photogenerated electron-hole pairs [5, 40]. However, an excessive amount of dopant can act as charge recombination centers. The optimal N doping amount in TiO_2 in this study was identified as the N/Ti mole ratio of 0.08 (0.1 NT).

3.3. Comparisons of Different Photocatalysts for BPA Degradation. Figures 10 and 11 show the effects of different photocatalysts on BPA removal rate under 410 nm visible-light and sunlight irradiation, respectively. The BPA photodegradation rate satisfies pseudo-first-order kinetics, and various studies

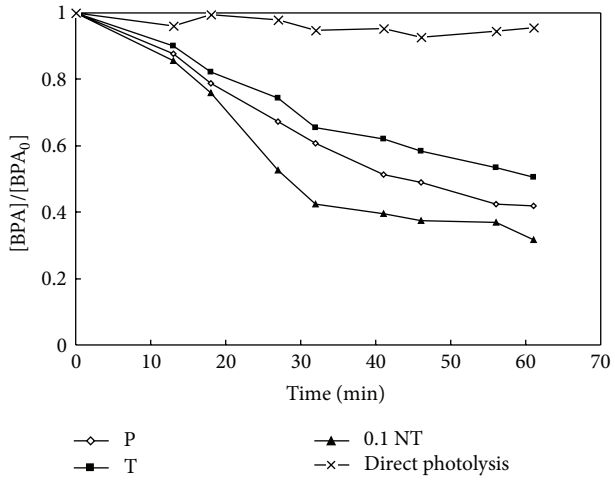

Figure 10: Photodegradation of BPA under 410 nm visible-light irradiation (BPA = 10 mg/L, pH = 6, and photocatalyst = 6.7 g/L).

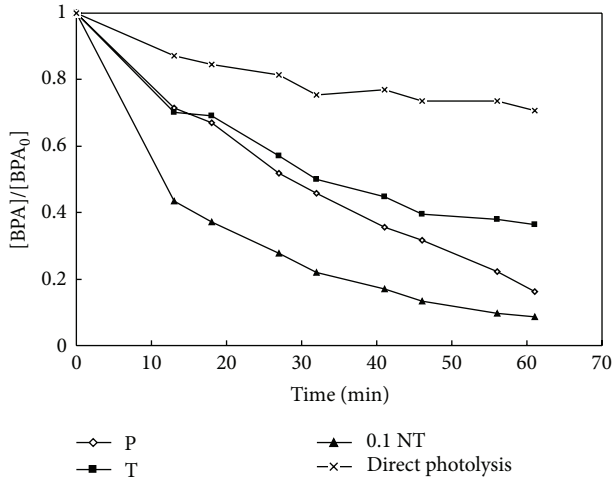

Figure 11: Photodegradation of BPA under sunlight irradiation (BPA = 10 mg/L, pH = 6, and photocatalyst = 6.7 g/L).

have demonstrated that photodegradation rates for organics can be approximated using pseudo-first-order kinetics [7, 16, 17]. The BPA photodegradation rate was 0.1 NT > P > T > photolysis for 410 nm visible-light and sunlight irradiation. The BPA photodegradation rate by sunlight irradiation was higher than that by 410 nm visible-light irradiation because the intensity of sunlight is greater than that of 410 nm visible light. Table 3 lists the pseudo-first-order rate constants (k) of BPA for different photocatalysts. Under 410 nm visible-light irradiation, k values were in the order of 0.1 NT > 0.05 NT > 0.2 NT > P > 0.5 NT > 1.5 NT > T. Photocatalytic activity was improved significantly by N doping. Yang et al. [17] demonstrated that BPA removal percentage of undoped TiO_2, Degussa P25, and N-TiO_2 under visible-light irradiation in a suspended system was 5%, 15%, and 30%, respectively, and the trend was similar to that in this study. Obviously, 0.1 NT had the fastest photodegradation rate and the highest removal percentage for BPA under both 410 nm visible-light and sunlight irradiation. Therefore, 0.1 NT was utilized to evaluate BPA mineralization. The BPA removal percentage for P and 0.1 NT was 58% and 68%, respectively; additionally, the TOC removal percentage for P and 0.1 NT was 4% and 41%, respectively. Experimental results indicate that 0.1 NT was the best photocatalyst for BPA and TOC degradation.

Table 3: The pseudo-first-order rate constants of BPA for different photocatalysts (BPA = 10 mg/L, pH = 6, and photocatalyst = 6.7 g/L).

	410 nm visible light		Sunlight	
	k (hr^{-1})	R^2	k (hr^{-1})	R^2
P	0.90	0.986	1.60	0.976
T	0.68	0.986	1.12	0.943
0.05 NT	1.13	0.948	1.89	0.960
0.1 NT	1.21	0.922	2.59	0.961
0.2 NT	1.06	0.993	1.43	0.929
0.5 NT	0.89	0.982	2.00	0.977
1.5 NT	0.73	0.983	0.83	0.936

Figure 12 lists the photocatalytic efficiency of repeated tests for P and 0.1 NT under 410 nm visible-light irradiation. The BPA removal of P in runs 1, 2, 3, 4, and 5 was 60%, 58%, 50%, 42%, and 39%, respectively; moreover, that of 0.1 NT was 68%, 66%, 59%, 52%, and 49%, respectively. Photocatalyst efficiency decreased as the number of repeats increased. The factor of (efficiency in run 5)/(efficiency in run 1) for P and 0.1 NT was 0.65 and 0.72, respectively. The performance of cyclic usability for 0.1 NT was greater than that for P. The concentration of released TiO_2 in effluent for 0.1 NT was 1.13 mg/L in run 1; additionally, no TiO_2 was released in effluent during runs 2–5. Experimental results demonstrate that 0.1 NT was the best photocatalyst, and visible-light-immobilized N-TiO_2 and sunlight-immobilized N-TiO_2 systems are suitable for BPA degradation. Additionally, visible-light-immobilized N-TiO_2 system was stable during photocatalytic degradation.

4. Conclusions

This investigation utilized N-TiO_2/glass immobilized beads to degrade BPA. The ratio of anatase in prepared N-TiO_2 increased as the N/Ti ratio increased; conversely, band gap energy decreased as the N/Ti ratio increased. Two forms of N-TiO_2, Ti–O–N and N–Ti–O, were identified by XPS analysis. The optimal N/Ti mole ratio was 0.08, and N doping synergistically served as electron traps that inhibited recombination of photogenerated electron-hole pairs. The BPA degradation efficiency increased as the photocatalyst dose increased; moreover, the photocatalytic activity of N-TiO_2 was higher under sunlight irradiation than under visible-light irradiation. The TOC removal percentage during BPA photodegradation was 0.1 NT > P. This study suggested that visible-light-immobilized N-TiO_2 and sunlight-immobilized N-TiO_2 systems are effective for BPA degradation. Moreover, the visible-light-immobilized N-TiO_2 system had a high cyclic efficacy for BPA photodegradation.

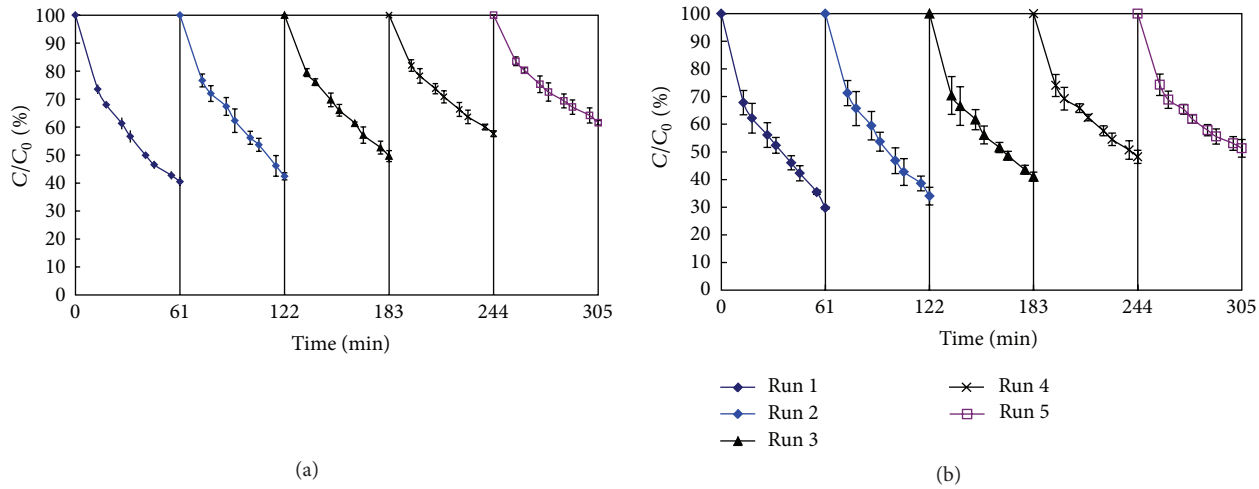

FIGURE 12: Photocatalytic efficiency of cyclic tests for (a) P and (b) 0.1 NT (BPA = 10 mg/L, pH = 6, 410 nm visible light, and photocatalyst = 6.7 g/L).

Acknowledgment

The authors would like to thank the National Science Council Taiwan, for financially supporting this research under Contract no. NSC 101–2221-E-151-038-MY3.

References

[1] C. A. Staples, P. B. Dorn, G. M. Klecka, S. T. O'Block, and L. R. Harris, "A review of the environmental fate, effects, and exposures of bisphenol A," *Chemosphere*, vol. 36, no. 10, pp. 2149–2173, 1998.

[2] J. A. Brotons, M. F. Olea-Serrano, M. Villalobos, V. Pedraza, and N. Olea, "Xenoestrogens released from lacquer coatings in food cans," *Environmental Health Perspectives*, vol. 103, no. 6, pp. 608–612, 1995.

[3] W. Ho, J. C. Yu, and S. Lee, "Low-temperature hydrothermal synthesis of S-doped TiO_2 with visible light photocatalytic activity," *Journal of Solid State Chemistry*, vol. 179, no. 4, pp. 1171–1176, 2006.

[4] L. Szatmáry, S. Bakardjieva, J. Subrt et al., "Sulphur doped nanoparticles of TiO_2," *Catalysis Today*, vol. 161, no. 1, pp. 23–28, 2011.

[5] R. Asahi, T. Morikawa, T. Ohwaki, K. Aoki, and Y. Taga, "Visible-light photocatalysis in nitrogen-doped titanium oxides," *Science*, vol. 293, no. 5528, pp. 269–271, 2001.

[6] R. Silveyra, L. T. Saenz, W. A. Flores, V. C. Martınez, and A. A. Elguezabal, "Doping of TiO_2 with nitrogen to modify the interval of photocatalytic activation towards visible radiation," *Catalysis Today*, vol. 107, pp. 602–605, 2005.

[7] Y. Ma, J. Zhang, B. Tian, F. Chen, and L. Wang, "Synthesis and characterization of thermally stable Sm,N co-doped TiO_2 with highly visible light activity," *Journal of Hazardous Materials*, vol. 182, no. 1–3, pp. 386–393, 2010.

[8] S. Irmak, O. Erbatur, and A. Akgerman, "Degradation of 17β-estradiol and bisphenol A in aqueous medium by using ozone and ozone/UV techniques," *Journal of Hazardous Materials*, vol. 126, no. 1–3, pp. 54–62, 2005.

[9] M. Debordea, S. Rabouana, P. Mazelliera, J. P. Duguetc, and B. Legubea, "Oxidation of bisphenol A by ozone in aqueous solution," *Water Research*, vol. 42, no. 16, pp. 4299–4308, 2008.

[10] T. Nakashima, Y. Ohko, D. A. Tryk, and A. Fujishima, "Decomposition of endocrine-disrupting chemicals in water by use of TiO_2 photocatalysts immobilized on polytetrafluoroethylene mesh sheets," *Journal of Photochemistry and Photobiology A*, vol. 151, no. 1–3, pp. 207–212, 2002.

[11] N. Watanabe, S. Horikoshi, H. Kawabe, Y. Sugie, J. Zhao, and H. Hidaka, "Photodegradation mechanism for bisphenol A at the TiO_2/H_2O interfaces," *Chemosphere*, vol. 52, no. 5, pp. 851–859, 2003.

[12] K. Chiang, T. M. Lim, L. Tsen, and C. C. Lee, "Photocatalytic degradation and mineralization of bisphenol A by TiO_2 and platinized TiO_2," *Applied Catalysis A*, vol. 261, no. 2, pp. 225–237, 2004.

[13] Y. B. Xie and X. Z. Li, "Degradation of bisphenol A in aqueous solution by H_2O_2-assisted photoelectrocatalytic oxidation," *Journal of Hazardous Materials*, vol. 138, no. 3, pp. 526–533, 2006.

[14] R. A. Torres-Palma, J. I. Nieto, E. Combet, C. Pétrier, and C. Pulgarin, "An innovative ultrasound, Fe^{2+} and TiO_2 photoassisted process for bisphenol a mineralization," *Water Research*, vol. 44, no. 7, pp. 2245–2252, 2010.

[15] R. Wang, D. Ren, S. Xia, Y. Zhang, and J. Zhao, "Photocatalytic degradation of Bisphenol A (BPA) using immobilized TiO_2 and UV illumination in a horizontal circulating bed photocatalytic reactor (HCBPR)," *Journal of Hazardous Materials*, vol. 169, no. 1–3, pp. 926–932, 2009.

[16] C. Y. Kuo, C. H. Wu, and H. Y. Lin, "Photocatalytic degradation of bisphenol A in a visible light/TiO_2 system," *Desalination*, vol. 256, no. 1–3, pp. 37–42, 2010.

[17] J. Yang, J. Dai, and J. Li, "Synthesis, characterization and degradation of Bisphenol A using Pr, N co-doped TiO_2 with highly visible light activity," *Applied Surface Science*, vol. 257, no. 21, pp. 8965–8973, 2011.

[18] S. Kaneco, M. A. Rahman, T. Suzuki, H. Katsumata, and K. Ohta, "Optimization of solar photocatalytic degradation conditions of bisphenol A in water using titanium dioxide,"

Journal of Photochemistry and Photobiology A, vol. 163, no. 3, pp. 419–424, 2004.

[19] B. Gao, T. M. Lim, D. P. Subagio, and T. T. Lim, "Zr-doped TiO_2 for enhanced photocatalytic degradation of bisphenol A," *Applied Catalysis A*, vol. 375, no. 1, pp. 107–115, 2010.

[20] H. Katsumata, S. Kawabe, S. Kaneco, T. Suzuki, and K. Ohta, "Degradation of bisphenol A in water by the photo-Fenton reaction," *Journal of Photochemistry and Photobiology A*, vol. 162, no. 2-3, pp. 297–305, 2004.

[21] I. Ioan, S. Wilson, E. Lundanes, and A. Neculai, "Comparison of Fenton and sono-Fenton bisphenol a degradation," *Journal of Hazardous Materials*, vol. 142, no. 1-2, pp. 555–558, 2007.

[22] M. Inoue, Y. Masuda, F. Okada, A. Sakurai, I. Takahashi, and M. Sakakibara, "Degradation of bisphenol A using sonochemical reactions," *Water Research*, vol. 42, no. 6-7, pp. 1379–1386, 2008.

[23] R. A. Torres, C. Pétrier, E. Combet, M. Carrier, and C. Pulgarin, "Ultrasonic cavitation applied to the treatment of bisphenol A. Effect of sonochemical parameters and analysis of BPA by-products," *Ultrasonics Sonochemistry*, vol. 15, no. 4, pp. 605–611, 2008.

[24] X. Wang and T. T. Lim, "Solvothermal synthesis of C-N codoped TiO_2 and photocatalytic evaluation for bisphenol A degradation using a visible-light irradiated LED photoreactor," *Applied Catalysis B*, vol. 100, no. 1-2, pp. 355–364, 2010.

[25] X. Wang and T. T. Lim, "Effect of hexamethylenetetramine on the visible-light photocatalytic activity of C-N codoped TiO_2 for bisphenol A degradation: evaluation of photocatalytic mechanism and solution toxicity," *Applied Catalysis A*, vol. 399, no. 1-2, pp. 233–241, 2011.

[26] D. V. Sojic, V. N. Despotovic, N. D. Abazovic, M. I. Comor, and B. F. Abramovic, "Photocatalytic degradation of selected herbicides in aqueous suspensions of doped titania under visible light irradiation," *Journal of Hazardous Materials*, vol. 179, no. 1–3, pp. 49–56, 2010.

[27] R. A. Spurr and H. Myers, "Quantitative analysis of anatase-rutile mixtures with an X-ray diffractometer," *Analytical Chemistry*, vol. 29, no. 5, pp. 760–762, 1957.

[28] S. Y. Liu, Q. L. Tang, and Q. G. Feng, "Synthesis of S/Cr doped mesoporous TiO_2 with high-active visible light degradation property via solid state reaction route," *Applied Surface Science*, vol. 257, no. 13, pp. 5544–5551, 2011.

[29] S. T. Hussain, K. Khan, and R. Hussain, "Size control synthesis of sulfur doped titanium dioxide (anatase) nanoparticles, its optical property and its photo catalytic reactivity for $CO_2 + H_2O$ conversion and phenol degradation," *Journal of Natural Gas Chemistry*, vol. 18, no. 4, pp. 383–391, 2009.

[30] Y. Wang, Y. Huang, W. Ho, L. Zhang, Z. Zou, and S. Lee, "Biomolecule-controlled hydrothermal synthesis of C-N-S-tridoped TiO_2 nanocrystalline photocatalysts for NO removal under simulated solar light irradiation," *Journal of Hazardous Materials*, vol. 169, no. 1–3, pp. 77–87, 2009.

[31] H. Li, J. Li, and Y. Huo, "Highly active TiO_2N photocatalysts prepared by treating TiO_2 precursors in NH_3/ethanol fluid under supercritical conditions," *The Journal of Physical Chemistry B*, vol. 110, no. 4, pp. 1559–1565, 2006.

[32] J. H. Xu, W. L. Dai, J. Li et al., "Simple fabrication of thermally stable apertured N-doped TiO_2 microtubes as a highly efficient photocatalyst under visible light irradiation," *Catalysis Communications*, vol. 9, no. 1, pp. 146–152, 2008.

[33] F. Cot, A. Larbot, G. Nabias, and L. Cot, "Preparation and characterization of colloidal solution derived crystallized titania powder," *Journal of the European Ceramic Society*, vol. 18, no. 14, pp. 2175–2181, 1998.

[34] S. Hu, A. Wang, X. Li, and H. Löwe, "Hydrothermal synthesis of well-dispersed ultrafine N-doped TiO_2 nanoparticles with enhanced photocatalytic activity under visible light," *Journal of Physics and Chemistry of Solids*, vol. 71, no. 3, pp. 156–162, 2010.

[35] C. Burda, Y. Lou, X. Chen, A. C. S. Samia, J. Stout, and J. L. Gole, "Enhanced nitrogen doping in TiO_2 nanoparticles," *Nano Letters*, vol. 3, no. 8, pp. 1049–1051, 2003.

[36] M. Xing, J. Zhang, and F. Chen, "New approaches to prepare nitrogen-doped TiO_2 photocatalysts and study on their photocatalytic activities in visible light," *Applied Catalysis B*, vol. 89, no. 3-4, pp. 563–569, 2009.

[37] M. Sathish, B. Viswanathan, R. P. Viswanath, and C. S. Gopinath, "Synthesis, characterization, electronic structure, and photocatalytic activity of nitrogen-doped TiO_2 nanocatalyst," *Chemistry of Materials*, vol. 17, no. 25, pp. 6349–6353, 2005.

[38] X. Chen and C. Burda, "Photoelectron spectroscopic investigation of nitrogen-doped titania nanoparticles," *The Journal of Physical Chemistry B*, vol. 108, no. 40, pp. 15446–15449, 2004.

[39] J. L. Gole, J. D. Stout, C. Burda, Y. Lou, and X. Chen, "Highly efficient formation of visible light tunable $TiO_{2-x}N_x$ photocatalysts and their transformation at the nanoscale," *The Journal of Physical Chemistry B*, vol. 108, no. 4, pp. 1230–1240, 2004.

[40] J. A. Rengifo-Herrera and C. Pulgarin, "Photocatalytic activity of N, S co-doped and N-doped commercial anatase TiO_2 powders towards phenol oxidation and *E. coli* inactivation under simulated solar light irradiation," *Solar Energy*, vol. 84, no. 1, pp. 37–43, 2010.